ELSEVIER

Journal of Photochemistry and Photobiology A: Chemistry 128 (1999) 111–120

Journal of Photochemistry and Photobiology A:Chemistry

www.elsevier.nl/locate/jphotochem

Synthesis and characterization of new chloride-sensitive indicator dyes based on dynamic fluorescence quenching

Christian Huber, Karsten Fähnrich, Christian Krause, Tobias Werner *

University of Regensburg, Institute of Analytical Chemistry, Chemo-and Biosensors, 93040 Regensburg, Germany

Received 30 June 1999; accepted 27 July 1999

Abstract

New water-soluble chloride-sensitive indicator dyes based on a bisacridine backbone were synthesized. These quaternized bisacridinium derivatives and the commercial available lucigenin are compared with acridinium compounds in terms of absorbance, fluorescence excitation and emission spectra, their fluorescence decay time and Stern-Volmer constants (K_{SV}) for quenching by a series of anions. All these dyes are quenched dynamically on exposure to chloride and obey the Stern-Volmer law. The effect of pH, buffer composition and ionic strength on the quenching mechanism was investigated. ©1999 Elsevier Science S.A. All rights reserved.

Keywords: Fluorescence quenching; Chloride probe; Bisacridinium derivatives

1. Introduction

The principle of dynamic fluorescence quenching is well-known. A wide variety of substances act as quenchers of fluorescence. One of the most investigated collisional quencher is molecular oxygen [1] and sensor applications are described in literature [2,3].

Dynamic (collisional) quenching results from diffusive encounters between the excited state fluorophore and the quencher [4]. The relationship between fluorescence intensity and the quencher concentration can be described by the Stern-Volmer equation (Eq. (1)).

$$\frac{F_0}{F} = 1 + k_q \cdot \tau_0 \cdot [\mathrm{Q}] = 1 + K_{\mathrm{SV}} \cdot [\mathrm{Q}] \quad (1)$$

F_0 and F are the fluorescence intensities in absence and presence of a quencher, [Q] is the concentration of the quencher, k_q is the bimolecular rate constant for quenching, τ_0 the lifetime of the excited state in absence of a quencher and K_{sv} is the Stern-Volmer quenching constant. It is important to mention that the observation of a linear Stern-Volmer plot does not prove that collisional quenching of fluorescence has occurred because static quenching displays also a linear plot. Static quenching, which is due to the formation of a non-fluorescent complex between the analyte and the fluorophore, is a frequent complicating factor in the analysis of dynamic quenching. The most effective way to distinguish between collisional and static quenching is the measurement of fluorescence decay time [4].

Quinolinium and acridinium compounds are well-studied fluorescent indicator dyes dynamically quenched by halides [5–8]. 3-Sulfopropylquinolinium (SPQ) has been used for the measurement of intracellular chloride activity and for analysis of chloride transport mechanisms in biological samples [9]. SPQ can be loaded into membrane vesicles and cells where it reports accurately the instantaneous chloride concentration or the exchange of chloride and bicarbonate across the human red cell membrane [10,11]. However, fluorescent chloride-sensitive indicators for bio-medical applications should be excitable at wavelength higher than 450 nm to avoid cellular autofluorescence, photodynamic cellular injury and apply the use of the cheap blue LED. Furthermore, they have to display high sensitivity and selectivity for chloride and possess high quantum yields, molar extinction and a large Stokes shift.

Lucigenin was mentioned to be effectively quenched by halides and amines [12,13]. The quenching of fluorescence of lucigenin by chloride and several anions was studied. Due to the advantageous properties of lucigenin new chloride-sensitive indicator dyes based on a bisacridinium backbone were synthesized and shown to have superior optical properties compared to quinolinium and acridinium compounds.

* Corresponding author. Tel.: +49-941-943-4015; fax: +49-941-943-4064
E-mail address: tobias.werner@chemie.uni-regensburg.de (T. Werner)

PII: S1010-6030(99)00160-4

2. Experimental

2.1. Chemicals

The chloride-sensitive dyes (*N*-(3-sulfopropyl)-acridinium) (SPA) and lucigenin were from Molecular Probes (Eugene, USA). *N*-(4-Nitrophenylbutyl)-acridinium 4′chlorobenzene-sulfonate (NPBA) was a friendly gift from AVL/List GmbH. 9,10 Dimethylacridinium methosulfate (DMA) was synthesized according to [14]. *N*-Methylacridinium-9-methylcarboxylate was synthesized according to Rauhut et al. [15,16].

All inorganic salts were of analytical grade (Merck, Darmstadt, Germany). 3-[*N*-Morpholin]-propane sulfonic acid and the respective sodium salt (MOPS), and *N*-2-hydroxyethylpiperazine-*N*′-2-ethanesulfonic acid (HEPES) were obtained from Sigma (Wien, Austria) and Serva (Heidelberg, Germany), respectively. The pH was adjusted using a sodium phosphate buffer $\left(c_{H_2PO_4^-} + c_{HPO_4^{2-}} = 5\,\text{mM}\right)$. The buffers were adjusted to constant ionic strength ($I = 210$ mM) using sodium fluoride as background electrolyte [17] unless other stated. Aqueous solutions were prepared from air-saturated double distilled water.

2.2. Instrumentation and measurements

Fluorescence excitation and emission spectra were acquired with an Aminco-Bowman Series 2 luminescence spectrometer (SLM-Aminco, Rochester, NY 14625, USA) equipped with a continuous wave 150 W xenon lamp as a light source. All fluorescence excitation and emission spectra were corrected. Absorbance was measured on a Hitachi (U-3000) UV-Vis spectrophotometer.

Fluorescence decay time measurements were carried out on an ISS K2 multifrequency phase-modulation fluorometer using a 150 W continuous xenon lamp (PS 300-1, ILC technology) as excitation light source and two signal generators (2022D from Maroni Instruments). The light was passed through a Pockels cell which provided modulated light. Emission was detected at 90° to the excitation through a convenient filter (bandpass filter with transmission at 445–495 nm, FITCA, and OG 550, Schott, Mainz, Germany). Lifetimes were referenced against a dilute solution of glycogen.

Elemental analyses (CHN) were carried out with a CHN-Rapid from Heraeus. Infrared spectra were received on a Perkin Elmer 881 infrared spectrometer. Mass spectra were acquired with a Varian MAT 311 A I (ei) and a Finnigan MAT 95 (fab). Melting points are uncorrected and were determined in open capillary tubes with a SMP-20 melting point apparatus from Büchi. Proton magnetic resonance spectra were recorded on a 250 MHz PFT-NMR spectrometer AC 250 from Bruker.

The pH values of the solutions were checked using a digital pH meter (Knick, Berlin, Germany) calibrated with standard buffers of pH 7.00 and 4.00 at 21 ± 1°C.

Dye concentrations for fluorescence excitation and emission and fluorescence decay time measurements were about 20 μM. Calibration curves were fitted with the Boltzmann function shown in Eq. (2).

$$\frac{F - F_0}{F_0} = \frac{Z - Y}{1 + \exp\,(\log\,(c/mM) - X/W)} + Y \qquad (2)$$

where *W*, *X*, *Y*, *Z* are empirical parameters describing the initial value (*Z*), final value (*Y*), center (*X*) and the width (*W*) of the fitting curve. The 50% decrease in fluorescence intensity [$c_{1/2}$ (Cl^-)] was calculated determining the point of inflection of the calibration curve. The Stern-Volmer constants (K_{SV}) were obtained by linear regression.

3. Synthesis

3.1. Methylacridinium (MAC)

A mixture of 1.5 mg (8.4 mM) acridine in 50 ml *p*-xylene and 1.5 ml (1.13 mg, 9 mM) dimethyl sulfate was heated to 100°C for 4 h. The mixture was cooled and the yellow residue was filtered off and was washed with xylole and ether. Yield: 0.9 g of yellow crystals (2.9 mM, 33%); Melting point: 192–196°C. Infrared spectrum (KBr): $\upsilon[cm^{-1}] = 3030, 3010, 2950, 1630, 1580, 1550, 1470, 1400, 1230, 1060, 1010, 870, 750$. ^{1}H-NMR ($D_2O$): $\delta = 9.72$ (s, 1H, aromatic), 8.41–8.47 (m, 4H, aromatic), 8.25–8.37 (m, 2H, aromatic), 7.83–7.89 (t, 2H, aromatic), 4.71 (s, 3H, CH_3O–SO_3^-), 3.64 (s, 3H, N–CH_3); Mass spectrum (ei, 70 eV) m/z (relative intensity): 194 (100 M^+); CHN-combustion analysis (in %): C: 58.7; H: 5.0; N: 4.6 (calculated for $C_{15}H_{15}NO_4S$ (305.35 g/mol): C: 59.0, H: 5.0, N: 4.6).

The synthetic strategy to obtain the quaternized bisacridinium derivatives is shown in Scheme 1.

3.2. Synthesis of acridone phosphorus oxychloride (4) [18,19]

A magnetically stirred solution of *N*-phenylanthranilic acid (1) (20 g, 93.8 mmol) in phosphorus oxychloride (70 ml, 118 g, 770 mmol) was carefully heated up to 80°C. A vigorous reaction started and the temperature was kept constant till the gas evolution stopped. Then, the mixture was refluxed for 2 h. The dark green solution was cooled in the refrigerator overnight. The yellow-green crystals were filtrated, washed with diethyl ether and dried in vacuum. 11.5 g (mmol) of (4a, 4b) were obtained and used in the next reaction without further purification.

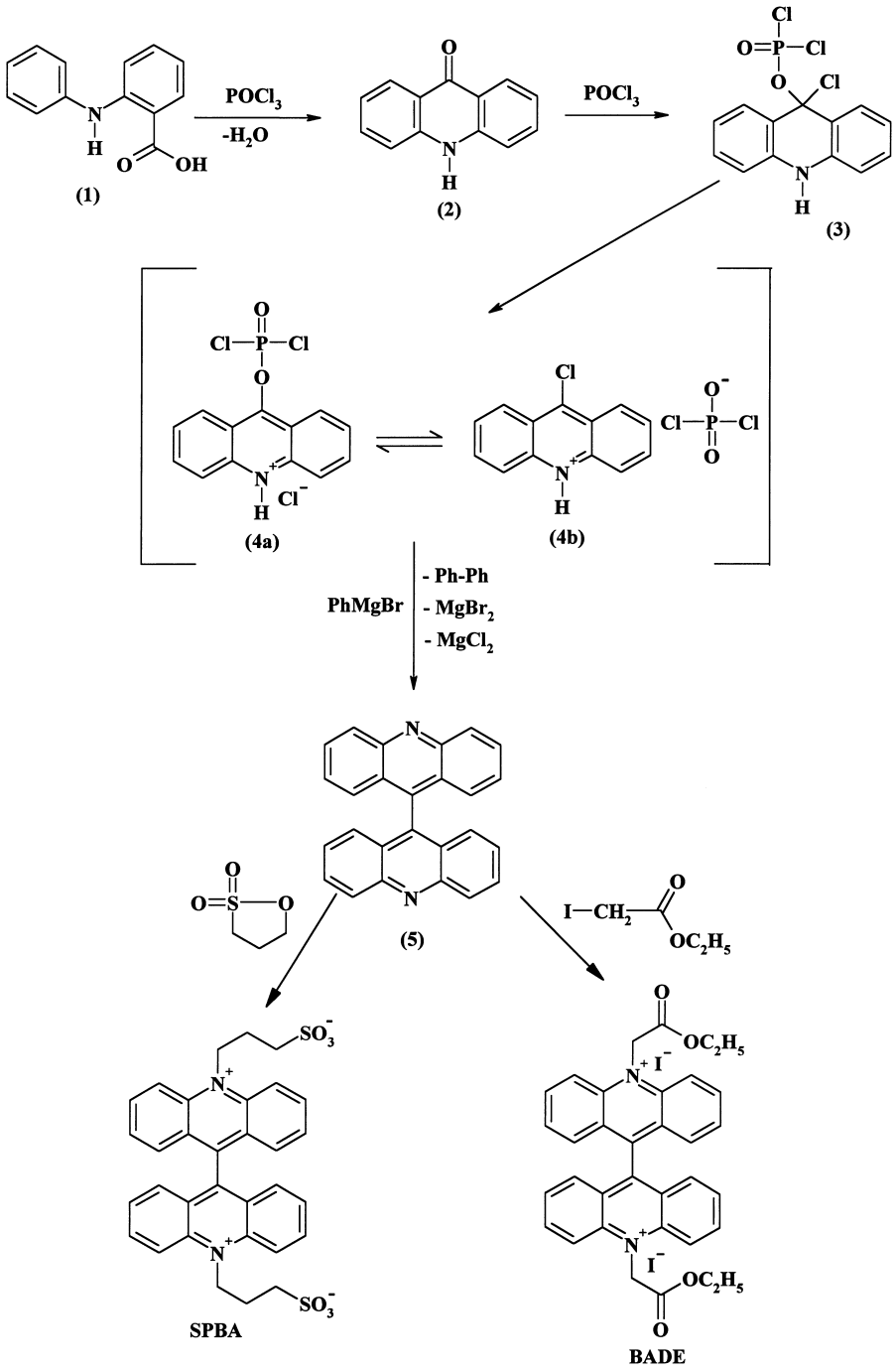

Scheme 1. Synthetic strategy of quaternized bisacridinium derivatives BADE and SPBA.

3.3. Synthesis of 9,9′-biacridine [20–22]

A solution of 56 g (357 mmol) of bromobenzene in 100 ml of absolute ether was prepared. Fifteen milliliter of this solution were added with a dropping funnel to a mixture of 8 g (329 mmol) of magnesium and 200 ml of absolute ether without stirring. Some iodine crystals were added turning the solution brown. The reaction mixture was slightly heated till the reaction started. This could be observed at the disappearance of the brown color. The remaining bromobenzene/ether solution was added dropwise over a period of 1 h under stirring. Afterwards, the solution was stirred for 15 min at room temperature. Then, the solution was refluxed for 15 min.

10.92 g (31.3 mmol) of acridone phosphorus oxychloride (4) were added slowly to the cooled Grignard solution, reacting vigorously. Afterwards, the mixture was refluxed for 15 min, cooled to room temperature and poured very slowly to a well stirred solution of 200 ml of water, 300 ml of 25% ammonia solution and 4 g of ammonium chloride. A vigorous reaction started, and a yellow precipitate arose. The

cold suspension was filtered, washed with water and dried in vacuum over phosphorus pentoxide. After recrystallization from toluene, 9,9′ biacridine was obtained. Yield: 3.2 g of yellow crystals (9 mmol, 30%); Melting point: >300°C. Infrared spectrum (KBr): υ[cm^{-1}] = 3446, 3054, 1631, 1610, 1550, 1515, 1460, 1439, 1404, 761, 750, 616; ^{1}H-NMR ($CDCl_3$): δ = 8.41 (d, 4H, aromatic, J = 8.9 Hz), 7.82 (m, 4H, aromatic), 7.36 (m, 4H, aromatic), 7.08 (d, 4H, aromatic, J = 9.4/0.7 Hz); Mass spectrum (ei, 70 eV) m/z (relative intensity): 356 (55 M^+), 264 (27), 219 (100), 169 (5); CHN-combustion analysis (in %): C: 87.1, H: 4.8, N: 7.8 (calculated for $C_{26}H_{16}N_2$ (356.4 g mol^{-1}): C: 87.5, H: 4.5, N: 7.9).

3.4. 9,9′-Bisacridinium-N,N′-di-aceticacidethylester (BADE)

Two hundred milligram (0.56 mmol) of bisacridine (5) and 1.5 ml (2.7 g, 12.6 mmol) iodoaceticacid-ethylester (6) were suspended in a sealed glass tube. The tube was heated to 110°C for 48 h. The crude residue was washed with ether to remove excess iodoaceticacid-ethylester. 9,9′-bisacridinium-*N*,*N*′-diaceticacidethylester (BADE) was extracted in water/methylene chloride several times and lyophilized. This procedure gives an effective product purification because the product is polar and water soluble while the reactants were nonpolar. The purity was confirmed by reverse phase thin layer chromatography. Yield: 0.03 g of brown crystals (0.03 mmol, 7%); Melting point: >300°C. Infrared spectrum (KBr): υ = 3060, 3020, 2960, 1740, 1630, 1610, 1550, 1450, 1260, 1230 cm^{-1}, ^{1}H-NMR (D_2O): δ = 8.57 (d, 4H, aromatic), 8.38 (t, 4H, aromatic), 7.65 (t, 4H, aromatic), 7.49 (d, 4H, aromatic), 4.39 (t, 4H, O–CH_2), 1.31 (t, 6H, CH_3–CH_2); Mass spectrum (ei, 70 eV) m/z (relative intensity): 531 (80, MH^+), 530 (76 M^{2+}), 443 (84), 415 (20); CHN-combustion analysis (in %): C: 56.1, H: 4.18, N: 2.82 (calculated for $C_{34}H_{30}N_2O_4I_2$ (784.4 g mol^{-1}): C: 52.1, H: 3.9, N: 3.6).

3.5. N,N-Di- (3-Sulfopropyl)-9, 9-bisacridinium (SPBA)

A mixture of 1 g (2.8 mmol) of 9,9-biacrinine (5) and 3.7 g (30.3 mmol) of 1,3-propanesultone (7) was stirred at 190°C in a pressure tube for 1 day. The crude brown substance dissolved in methanol was purified by reversed phase chromatography using silica gel and methanol as solvent. Yield: 200 mg (0.3 mmol, 12%) of yellow-brown crystals; Melting point: 270°C (decomposition); Infrared spectrum (KBr): 3434, 2921, 2853, 2366, 2342, 1612, 1550, 1468, 1449, 1383, 1193, 1044, 768 cm^{-1}; ^{1}H-NMR(D_2O): δ = 8.79 (d, 4H, aromatic), 8.37 (m, 4H, aromatic), 7.63 (m, 4H, aromatic), 7.35 (m, 4H, aromatic), 5.73 (m, 4H, CH_2–N), 3.35 (t, 4H, CH_2–SO_3^-), 2.81–2.71 (m, 4H, N–CH_2–CH_2–CH_2–SO_3^-); Mass spectrum (fab) m/z: 603.5 (93, MH_2^{2+}), 602.5 (100, MH^+), 479.4 (20) [23].

4. Results and discussion

4.1. Synthesis

9-Methylacridine (MAC) was synthesized by methylation of acridine with dimethyl sulfate. *N*-Methylacridinium-9-methylcarboxylate (MAMC) was synthesized by converting acridine-9-carboxylic acid to the acid chloride, followed by a reaction with methanol and a methylation of the heterocyclic nitrogen with dimethyl sulfate [15,16]. The synthetic strategy of the bisacridiniuin derivatives is shown in Scheme 1. (4) is prepared by a ring closure reaction of *N*-phenylanthranilic acid (1) in phosphoryl chloride. The exact characterization of (4) is not possible, both forms, (4a) and (4b) may be possible. However, as long as the yellow-green crystals of (4) are not out of the solution, no problem with hydrolysis to acridone occurs. The reductive coupling is carried out by adding (4) to a freshly prepared Grignard solution of bromobenzene and magnesium in ether. After hydrolysis and recrystallization with toluene the 9,9′-bisacridine (5) is obtained. The quaternization of (5) can be performed with iodoaceticacid-ethylester to obtain BADE or with propane sultone to obtain SPBA.

4.2. Spectroscopic measurements

Fig. 1 shows the chemical structures of the chloride-sensitive fluorescent indicator dyes. Their spectroscopic properties, including peak absorption (λ_{abs}), the molar extinction coefficient (ε), excitation and emission maxima ($\lambda_{ex}/\lambda_{em}$), fluorescence quantum yield (Φ) and their decay time (τ), are listed in Table 1. All bisacridinium derivatives have an excitation peak beyond 450 nm.

The fluorescence decrease of an air-saturated aqueous buffer solution of BADE at various chloride concentrations is shown in Fig. 2. As predicted for a dynamic quencher, the shape of the emission spectra and the absorption spectra are not altered by the addition of chloride.

Table 1
Spectroscopic properties of chloride-sensitive indicators

Compound	λ_{abs}[a] (nm)	ε[b] (M^{-1} cm^{-1})	$\lambda_{ex}/\lambda_{em}$ (nm)	Φ[c]	τ (ns)
SPA	357, 417	19700; 4000	359, 419/492	0.89	31.4
MAC	357, 415	18600; 3400	358, 419/492	0.87	33.3
NPBA	358, 418	19200; 3900	358, 419/492	0.83	31.4
DMA	357, 418	17400; 4300	357, 419/492	0.91	30.0
MAMC	366, 424	14500; 3200	367, 424/520	0.24	13.8
Lucigenin	368, 455	34800; 7200	369, 455/510	0.67	20.0
BADE	370, 462	29100; 5700	371, 467/525	0.35	12.2
SPBA	369, 460	31000; 7300	369, 460/515	0.52	18.0

[a] Absorbance peaks with maximum absorbance and longest wavelength are given.

[b] Molar extinction coefficient determined using the Lambert-Beer law measured at peak absorbance.

[c] Quantum yields were determined using lucigenin as standard.

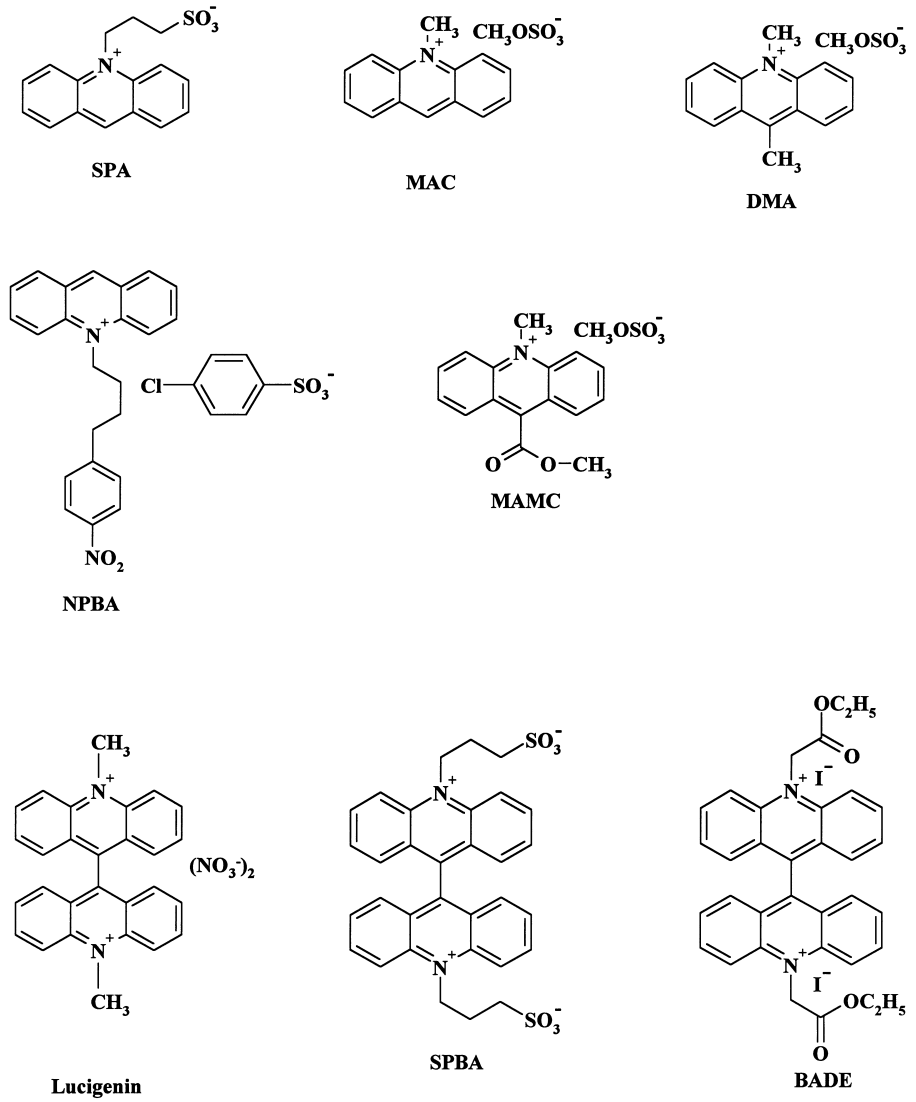

Fig. 1. Chloride-sensitive indicator dyes.

For each compound quenching by chloride occurred by a collisional mechanism as judged by the parallel decrease in fluorescence intensity and decay time on addition of chloride. In an aqueous solution the dyes exhibit a mono-exponential fluorescence decay time which is listed in Table 1. In the presence of chloride, the decay time of the dyes remained mono-exponential but decreases. Fig. 3 shows the equivalent increase of $I_0/I-1$ and $\tau_0/\tau-1$ with the chloride concentration and hence excludes static quenching by complex formation between the indicator and chloride.

Fluorescence of each compound is not markedly affected by phosphate (used as buffer component), fluoride, and pH in the range 4–8. Fig. 4 shows the calibration plots of BADE for chloride, bromide, iodide, sulfate and nitrate, respectively. As supposed bromide and iodide show a pronounced quenching effect on the fluorescence. The effective quenching for bromide and especially for iodide has been attributed to a charge-transfer interaction between excited fluorophore and bromide or iodide, since the much lower ionization potential of the higher halides.

The titration plots shown in Fig. 4 cannot differentiate between dynamic quenching and other quenching effects. Concerning the fluorescence intensities, linear Stern-Volmer plots are only obtained at concentrations <25 mM for bromide and iodide. At concentrations >25 mM Stern-Volmer plots showed upward curvature indicating a further quenching process. The dynamic quenching constant (K_{SV}) can be determined by decay time measurements. Indeed, linear Stern-Volmer plots were obtained as can be seen in Fig. 4. In dynamic quenching sometimes an additional static quenching can be observed in the case of high quencher concentrations. The combined quenching recognized by the upward curvature of the Stern-Volmer plot can be expressed by a modified Stern-Volmer Eq. (3).

$$\frac{F_0}{F} = (1 + K_{SV}[Q]) \cdot (1 + K_S[Q]) \quad (3)$$

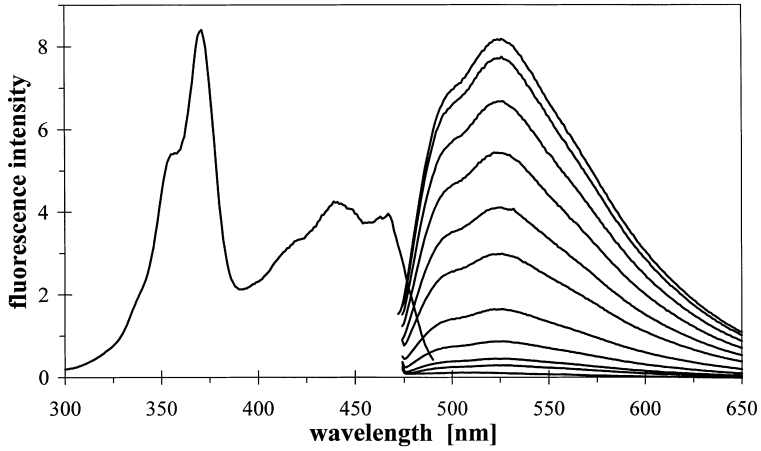

Fig. 2. Fluorescence excitation and emission spectra of BADE ($c = 20\ \mu M$), excited at 466 nm. The chloride concentrations are (in order of decreasing intensity) 0, 0.2, 1, 2, 4, 10, 25, 50, 100, 160, and 200 mM.

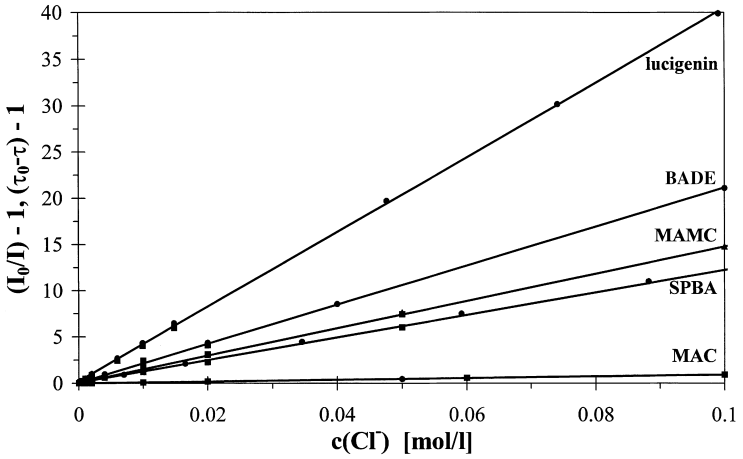

Fig. 3. Stern-Volmer plots for quenching of lucigenin, BADE, MAMC, SPBA, and MAC. All *r*-values are generally >0.997. Scales on the ordinate are $F_0/F-1$ [●] and $\tau_0/\tau-1$ [■].

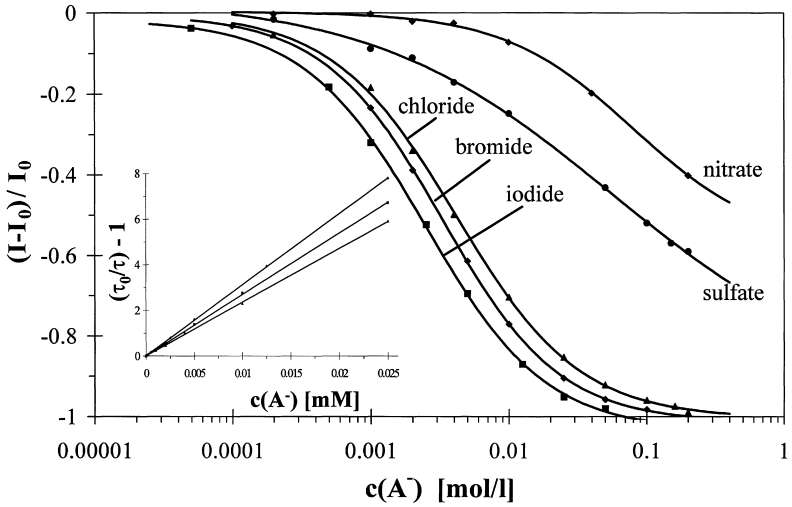

Fig. 4. Calibration plots of BADE for chloride, bromide, iodide, salicylate, nitrate and sulfate. Stern-Volmer plots for chloride, bromide and iodide are inserted.

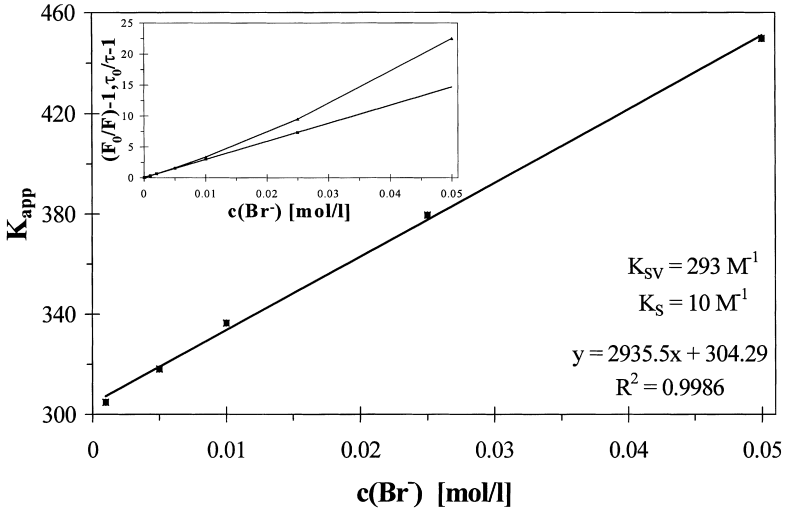

Fig. 5. Determination of dynamic and static quenching constants by a linear plot of K_{app} vs. [Q]. The upward curvature from the linear Stern-Volmer plot concerning fluorescence intensities at higher quencher concentrations is inserted.

Table 2
Stern-Volmer constants for quenching of fluorescence in a 5 mM phosphate buffer solution by a series of anions. The correlation coefficients generally are higher than $r > 0.997$

Indicator	K_{SV} (Cl^-) (M^{-1}) $c_{1/2}(Cl^-)$ (mM)	K_{SV} (Br^-) (M^{-1}) $c_{1/2}(Br^-)$ (mM)	K_{SV} (I^-) (M^{-1}) $c_{1/2}(I^-)$ (mM)	K_{SV} (NO_3^-) (M^{-1}) $c_{1/2}(NO_3^-)$ (mM)	K_{SV} (SO_4^{2-}) [M^{-1}] $c_{1/2}(SO_4^{2-})$ (mM)
SPA	8 67	280 6.6	360 5.4	0 –[a]	0 –
MAC	8.7 94	466 2.4	615 2	0 –	0 –
DMA	1 –	510 2.1	744 1.6	0 –	0 –
NPBA	8.7 56.9	483 2.2	802 1.9	0 –	0 –
MAMC	148 5.5	244 3.7	418 2.9	1 –	0 –
Lucigenin	390 2.4	533 1.8	600 1.7	2 128	5[b] –
SPBA	124 7.3	209 4.9	271 3.2	2.1 259	3.3 243
BADE	237 4.0	292 3.3	312 2.5	3 –	8.4[b] 40

[a] Not determinable.
[b] No linearity.

where K_S is the complex formation constant of the fluorophore-quencher complex. Eq. (3) can be simplified to Eq. (4) by introducing an apparent constant K_{app}, measured for various analyte concentrations.

$$\frac{F_0}{F} - 1 = [(K_{SV} + K_S) + K_{SV}K_S[Q]] \cdot [Q] = K_{app}[Q] \quad (4)$$

A plot of K_{app} versus [Q] yields a straight line with the slope $S = K_{SV}{*}K_S$ and an intercept $I = K_{SV} + K_S$ (Fig. 5).

The Stern-Volmer constant of BADE for bromide determined by fluorescence decay time analysis is 294 M^{-1}. Indeed, calculating the Stern-Volmer constant (K_{SV}) by means of Eq. (4) yields 293 M^{-1} agreeing with the K_{SV} value obtained via decay time measurement. Additional, a second solution was obtained corresponding to the complex formation constant (K_S) which is 10 M^{-1}. However, the upward curvature for iodide cannot be attributed to an additional static quenching since no linear plot of K_{app} versus [Q] is obtained. Iodide is known to quench fluorescence due to the heavy atom-effect through a spin-orbit coupling in the

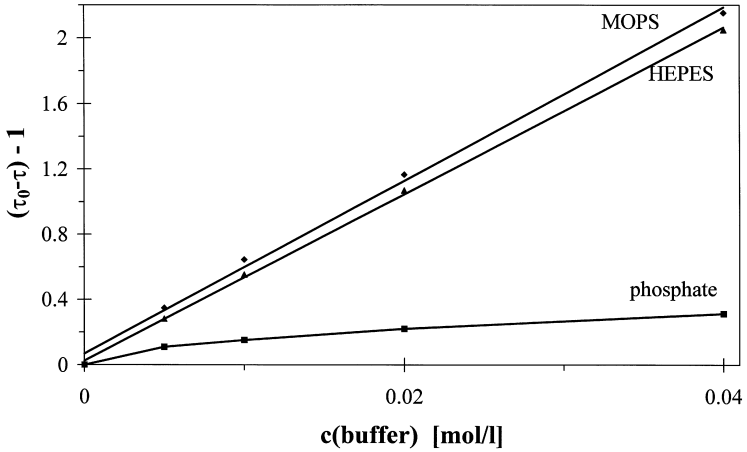

Fig. 6. Dynamic quenching of lucigenin fluorescence by MOPS, HEPES, and phosphate.

encounter complex of excited fluorophore and the iodide [24] which may be the reason for the upward curvature. The Stern-Volmer constants, obtained from the fitted line slopes, and the $c_{1/2}(A^-)$ values indicating the concentration where 50% of fluorescence is quenched, are summarized in Table 2.

The efficacy of dynamic quenching of acridinium derivatives strongly depends on the substituent at the 9-position [6]. Two different 9-substituted acridinium compounds were investigated, the one containing an electron-donating methyl group (DMA), the other an electron-withdrawing carboxylate group (MAMC). As can be seen, the sensitivity to chloride of these acridinium derivatives, which differ only in the substituent at the 9-position, are completely different. The Stern-Volmer constant of MAMC for chloride is $148\,M^{-1}$ while DMA is nearly insensitive to chloride ($K_{SV} = 1\,M^{-1}$). Obviously, stabilizing the positive charge of the nitrogen by inserting substituents with electron donating properties at the 9-position leads to chloride-insensitive compounds. However, it has been reported that the 9-position of acridine is electron deficient and suspect to nucleophilic attack at this position [25]. Consequently, the reactivity of this position is increased when substituted with an electron withdrawing group. MAMC was reported to be converted to 9-hydroxy-10-methylacridane-9-methylcaroxylate by addition of a hydroxyl group at the 9 position [26]. Fluorescence shifts from green to blue displaying a *N*-methylacridone similar spectrum, and hence, loosing its chloride-sensitivity. Because of the reactivity at the 9-position of MAMC and the low chloride-sensitivity of DMA, MAC and NPBA, these acridinium derivatives are not further investigated.

The Stern-Volmer constant (K_{SV}) is affected by the ionic strength [27]. Quenching efficiency becomes smaller, if the ionic strength of the solution increases. Dissolving the dyes in a 5 mM phosphate solution (pH 7.1) and adjusting the ionic strength to 210 mM by adding the respective amounts of sodium fluoride the Stern-Volmer constants decreases as can be seen in Table 3. This can be attributed to the decreased probability of a collisional process because a high concentration of background electrolyte tends to screen the positive charge of the bis-acridinium moiety.

Table 3
Stern-Volmer constants of anions in a 5 mM phosphate buffer solution containing a constant ionic strength of 200 mM

Indicator	K_{SV} (Cl^-) (M^{-1}) $c_{1/2}(Cl^-)$ (mM)	$K_{SV}(Br^-)$ (M^{-1}) $c_{1/2}(Br^-)$ (mM)	$K_{SV}(I^-)$ (M^{-1}) $c_{1/2}(I^-)$ (mM)
SPA	6.6	309	392
	152	4.3	3.7
Lucigenin	174	300	469
	6.3	4.5	2.6
SPBA	90	198	260
	13.6	7.4	5
BADE	123	173	254
	9.6	6.5	4.2

Table 4
Stern-Volmer constants of lucigenin for various buffer components

Buffer components (pH 7.1)	$K_{sv}[M^{-1}]$
Na_2HPO_4/NaH_2PO_4	7.7 (0.8332)[a]
MOPS-sodium salt	53 (0.995)[a]
HEPES-1 M NaOH	51 (0.997)[a]

[a] R^2 value (correlation coefficient).

4.3. Buffer-dependent fluorescence quenching of lucigenin

The lifetime data of lucigenin in a phosphate buffer, 3-[*N*-morpholino]propane sulfonic acid (MOPS) buffer, and *N*-2-hydroxyethylpiperazine-*N*′-2-ethanesulfonic acid (HEPES) of various concentrations adjusted to pH 7.1 were tested. The quenching of fluorescence of 6-methoxy-*N*-(3-sulfopropyl)quinolinium (SPQ) by HEPES was recently described in the literature [11,28]. We found that both HEPES and MOPS quench the fluorescence of lucigenin. The decay time data are plotted as a Stern-Volmer plot in Fig. 6. The linearity of the plot indicates collisional quenching with Stern-Volmer quenching constants of 61 and $58\,M^{-1}$, respectively. The results are summarized in Table 4.

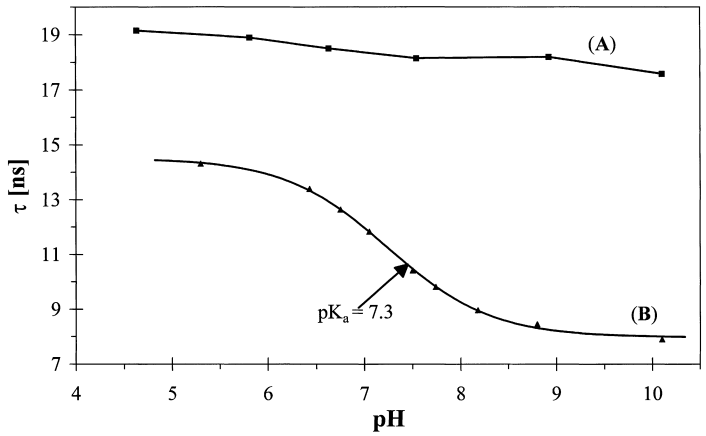

Fig. 7. pH calibration plot of a 20 μM lucigenin solution. The pH values are adjusted (A) with NaH_2PO_4/Na_2HPO_4, and (B) HEPES/1 M NaOH.

The decrease in fluorescence decay time on exposure to phosphate buffers of various concentrations did not obey the Stern-Volmer law. This deviation from the linear Stern-Volmer plot indicates that the quenching mechanism is more complex than a simple bimolecular collisional mechanism.

Fig. 7 shows the pH titration plot of lucigenin dissolved either in a phosphate buffer or HEPES buffer. Fluorescence of lucigenin is insensitive to pH adjusting it with a phosphate buffer. The fluorescence decay time decreases about 1 ns in the pH range of 4–10 which is referred to the small quenching effect of OH^- ions. The situation is completely different observing the pH dependence adding a HEPES buffer. An aqueous solution of lucigenin with a buffer consisting of 10 mM *N*-2-hydroxyethylpiperazine-*N*′-2-ethanesulfonic acid (HEPES) decreases the fluorescence decay time to 14.3 ns. Increasing pH by adding 1 M sodium hydroxide solution results in a further decrease in fluorescence decay time what is attributed to the different quenchability of lucigenin by molecular HEPES and its sodium salt built by increasing pH. Indeed, the pH titration curve in Fig. 7 gives a pK_a of 7.3 which is very similar to that of HEPES (7.55).

5. Conclusion

A series of bisacridinium and acridinium compounds were synthesized and investigated in terms of their spectral properties and quenching constants by several anions. Substitution of the 9-position with groups having electron-withdrawing properties (MAMC) yields much higher chloride sensitivity than acridinium derivatives having no (SPA, MAC, NPBA) or an electron-donating substituent (DMA) at this position. The bisacridinium derivatives lucigenin, BADE and SPBA are shown to be superior to the acridinium derivatives. They are strongly quenched by chloride in a collisional manner and display a better selectivity to chloride than acridinium derivatives. They can be excited at wavelength of 450 nm or higher and therefore are compatible to the cheap blue LED and avoid autofluorescence of biological samples. Quenching of fluorescence by bromide and iodide deviates from the linear Stern-Volmer plot indicating additional quenching processes, such as static quenching. Fluorescence is hardly quenched by fluoride, nitrate, sulfate, and pH in the range of 4–10. However, organic buffers like HEPES and MOPS display distinct dynamic quenching.

Acknowledgements

The authors want to thank Ms. Hannelore Brunner and Mr. Berghausen for technical assistance.

References

[1] H. Kautsky, Quenching of luminescence by oxygen, Trans. Faraday Soc. 35 (1939) 216–219.
[2] D.B. Papkovsky, G.V. Ponomarev, W. Trettnak, P. O'Leary, Phosphorescent complexes of porphyrin ketones: optical properties and application to oxygen sensing, Anal. Chem. 67 (1995) 4112–4117.
[3] O.S. Wolfbeis, Oxygen Sensors, in Fiber Optic Chemical Sensors and Biosensors, Chap. 9, CRC Press, Boca Raton, FL, 1991.
[4] J.R. Lakowicz, Principles of Fluorescence Spectroscopy, Plenum Press, New York and London, 1983.
[5] E. Urbano, H. Offenbacher, O.S. Wolfbeis, Optical sensor for continuous determination of halides, Anal. Chem. 56 (1984) 427–429.
[6] J. Biwersi, B. Tulk, A.S. Verkman, Long wavelength chloride-sensitive fluorescent indicators, Anal. Biochem. 219 (1994) 139–143.
[7] H. Burrows, S.J. Formosinho, M. Fernandia, J.R. Paiva, Halide ion induced quenching and enhancement of the fluorescence of fluoranthene solubilized in cetyltrimethylammonium bromide (CTAB) micelles, J. C. S. Faraday II 76 (1980) 685–692.
[8] A.S. Verkman, Development and biological applications of chloride-sensitive fluorescent indicators, Am. J. Physiol. 159 (1990) C375–C387.
[9] A.S. Verkman, M.C. Sellers, A.C. Chao, T. Leung, R. Ketcham, Synthesis and characterisation of improved chloride-sensitive

fluorescent indicators for biological applications, Anal. Biochem. 178 (1989) 355–361.
[10] N.P. Illsley, A.S. Verkman, Membrane chloride transport measured using a chloride-sensitive fluorescent probe, Biochemistry 26 (1987) 1215–1219.
[11] T.M. Calatful, J.A. Dix, Chloride-bicarbonate exchange through the human red cell ghost membrane monitored by the fluorescent probe, 6-methoxy-*N*-(3 sulfopropyl)quinolinium) (SPQ), Anal. Biochem. 230 (1995) 1–7.
[12] K. Legg, D.M. Hercules, Quenching of lucigenin fluorescence, J. Phys. Chem. 74 (1970) 2114–2118.
[13] A.E. Mantaka-Marketou, F.S. Varveri, G. Vassillopoulos, J. Nikokavouras, Some aspects of the lucigenin light reaction, J. Photochem. Photobiol. 48 (1989) 337–340.
[14] S. Hünig, O. Rosenthal, Farbe und Konstitution II, Phenolbetainfarbstoffe, Justus Liebigs Annalen der Chemie 592 (1955) 161–179.
[15] E. Rapaport, M.W. Cass, E.H. White, Chemiluminescence of linear hydrazides, J. Am. Chem. Soc. 94 (1972) 3153–3159.
[16] M. Rauhut, D. Seehan, R.H. Clarke, B.G. Roberts, A.M. Semsel, Chemiluminescence from the reaction of 9-Chlorocarbonyl-10-methylacridinium chloride with aqueous hydrogen peroxide, J. Org. Chem. 30 (1965) 3587–3592.
[17] D.D. Perrin, B. Dempsey, Buffers for pH and metal ion control, Chapman and Hall Laboratory Manuals, London, 1974.
[18] K. Gleu, S. Nitzsche, A. Schubert, Die Einwirkung von Phosphoroxychlorid und Oxalchlorid auf Acridone, Chem. Ber. 72 (1939) 1093–1099.
[19] G.D. Jaycox, G.W. Gribble, M.P. Hacker, Potential DNA bis-intercalating agents: synthesis and antitumor activity of novel, conformationally restricted bis(9-Aminoacridines), J. Heterocyclic Chem. 24 (1987) 1405–1408.
[20] K. Gleu, A. Schubert, Die Umsetzung der Phosphoroxy-chlorid-Acridone mit Grignard-Verbindungen, Chem. Ber. 73 (1940) 805–811.
[21] P. Kyriakos, J. Nikokavouras, D. Dimotikali, Reaction of lucigenin in protic solvents in the presence of amines, J. Prakt. Chem. 336 (1994) 506–508.
[22] K. Nakamaru, S. Niizuma, M. Koizumi, Photochemical reaction of 9-Cl-acridine in aerated and deaerated ethanol I, Bull. Chem. Soc. 44 (1971) 1256–1261.
[23] T. Werner, K. Fähnrich, Ch. Huber, O.S. Wolfbeis, Anion induced fluorescence quenching of a zwitterionic biacridine derivative, Photochem. Photobiol. (1999), in press.
[24] M. Kaska, Collisional perturbation of spin orbital coupling and the mechanism of fluorescence quenching. A visional demonstration of the perturbation, J. Chem. Phys. 20 (1952) 71–74.
[25] A. Selby, in: R.M. Acheson (Ed.), Acridines, Wiley, New York, 1973, pp. 433–443.
[26] M.W. Cass, E. Rapaport, E.H. White, Chemiluminescent reaction of 9-Caboxy-*N*-methylacridinium chloride with potassium peroxodisulfate, J. Am. Chem. Soc. 94 (1972) 3168–3175.
[27] R.I. Cukier, On the quencher concentration dependence of fluorescence quenching: the role of solution dielectric constant and ionic strength, J. Am. Chem. Soc. 107 (1985) 4115–4117.
[28] M. Vasseur, R. Frangne, Buffer-dependent pH sensitivity of the fluorescent chloride-indicator dye SPQ, Am. J. Physiol. 264 (1993) C27–C31.